Bose glass melting and the transverse Meissner effect in $YBa_2Cu_3O_{7-\delta}$ single crystals

A. W. Smith, H. M. Jaeger, and T. F. Rosenbaum
The James Franck Institute and Department of Physics, The University of Chicago, Chicago, Illinois 60637

W. K. Kwok and G. W. Crabtree
Materials Science Division, Argonne National Laboratory, Argonne, Illinois 60439

(Received 13 March 2000; revised manuscript received 20 June 2000; published 23 January 2001)

We map out the phase boundary separating the vortex solid and liquid phases in $YBa_2Cu_3O_{7-\delta}$ (YBCO) single crystals with irradiation-induced columnar defects. These randomly distributed, extended defects are expected to localize vortices into a ''Bose glass'' phase. The transition from the vortex liquid into the Bose glass is predicted to exhibit two fundamental signatures: a vanishing of the linear resistivity and, concomitantly, a screening of dc magnetic fields applied perpendicular to the defect axis, the transverse Meissner effect. We have investigated both aspects by systematic measurements on two YBCO single crystals with different defect densities (matching fields of 0.25 and 0.5 T), as well as on an unirradiated control sample. The melting line determined by the temperature, T_m, of vanishing resistance undergoes a 30% decrease in slope as the magnetic field is ramped through the matching field. This is evidence that interstitial vortices are pinned much more weakly than originally thought. If we associate the melting temperature with the Bose glass transition temperature, we obtain static critical exponents of $\nu_\perp = 1.7 \pm 0.2$ and $\nu_\perp = 1.9 \pm 0.1$ for the crystals with matching fields of 0.25 and 0.5 T, respectively. Simultaneously, we use a ten-element, linear array of microfabricated Hall probe magnetometers to observe directly the flux screening associated with the transverse Meissner state. We find the temperature above which the Meissner state breaks down, T_s, to decrease linearly as the magnetic field applied perpendicular to the columnar defect axis increases. This linear trend, found in both irradiated crystals to cover a range of at least 40 K in T_s, is closely in line with the current theoretical expectation $\nu_\perp \simeq 1$. However, already for angles as small as one degree, $T_s(H_\perp)$ falls below $T_m(H_\perp)$ by more than 10 K. Thus, between $T_s(H_\perp)$ and $T_m(H_\perp)$ we observe a large regime characterized by zero resistivity in the absence of a transverse Meissner effect: vortices remain effectively localized even when rotated off the columnar defects.

DOI: 10.1103/PhysRevB.63.064514 PACS number(s): 74.25.Bt, 74.60.Ge

I. INTRODUCTION

High-temperature superconductors are able to host a vortex liquid phase in addition to the vortex solid found in conventional superconductors due to their large anisotropy and thermal fluctuations.[1] In high quality single crystals with few pinning defects,[2] the vortex liquid was found to freeze into an ordered crystal in a first order phase transition. The effect of point disorder on the melting transition is dramatic, destroying the first order transition[3–5] and inducing a glassy state that is predicted to melt in a second or higher order transition.[6] In this paper, we consider the limit of much stronger disorder caused by defects that are randomly placed in a plane but spatially extend along the third dimension. In this case a transition is predicted from the vortex liquid into a Bose glass phase.[7] The Bose glass transition is thought to occur generically in disordered, two-dimensional (2D) systems with bosonic degrees of freedom, describing the transition between a superconducting or superfluid phase (the liquid state for the vortex system) and an insulating or solidlike phase (the Bose glass). New findings concerning the nature of the Bose-glass transition in the vortex system therefore may have profound implications for our understanding of the generalized, 2D superconductor-to-insulator phase transition. This paper discusses two primary experimental findings: first, the observation that correlated disorder affects the shape of the phase boundary in a qualitatively different way than predicted by theory; and second, the discovery of another phase of vortex matter extending far below the melting line usually associated with the onset of the Bose glass phase. The model system of ''vortex matter,'' used to illuminate problems ranging from dislocation motion in metals to dynamic phase transitions, provides fresh perspectives on the role of disorder in correlated materials.

Perhaps the strongest disorder possible in a vortex system arises from the randomly placed amorphous damage tracks created by heavy ion bombardment. These defects are of nearly optimal size for pinning, extend spatially over long distances, and potentially can localize vortices over their entire length. In spite of this, at any nonzero temperature some segment of a vortex line is thermally excited off its pinning site. Nelson and Vinokur[7] (NV) have mapped this statistical mechanics problem onto the quantum mechanical problem of 2D bosons in the presence of random point disorder.[8] In this analogy, the direction along the columnar defects is mapped onto imaginary time so that vortices become the world lines of 2D bosons, and temperature is mapped onto Planck's constant. NV argue for the existence of a sharp phase transition separating a high-temperature liquid phase of delocalized and entangled vortices from a low temperature Bose glass phase dominated by the spatial disorder in the columnar defect distribution. Conventionally, the theory is tested by measuring the mobility of vortices subjected to a driving current.[9–19] Scaling arguments[7,20–22] then predict how the

vortices slow down as the glass temperature is approached from above. These experiments vary widely on values for the critical exponents. In this paper, we test directly the second cornerstone of the theory, namely the prediction that the vortices should remain parallel to the columnar defects even as the external magnetic field is rotated. While this so-called transverse Meissner effect is a crucial element of the theory it so far has been untapped experimentally as a quantitative probe of the Bose glass state.[23]

The paper is organized as follows. In Sec. II we introduce the experimental setup, and describe the sample preparation and measurement procedure. For all samples, we performed two independent types of experiments, one aimed at elucidating the shape of the melting line, and one configured to map out the phase boundary for the transverse Meissner effect. Section III contains our experimental results for the melting line, while Sec. IV focuses on the transverse Meissner effect. Both aspects of the Bose glass transition are then compared and discussed in Sec. V, where we conclude with an outlook on the implications of our findings.

II. EXPERIMENTAL SETUP AND PROCEDURE

With the experimental apparatus sketched in Fig. 1, it is possible to measure both vortex motion in response to an external drive and vortex rotation relative to the columnar defects. We sense vortex mobility using a pickup coil near the sample. Since each vortex carries a fixed amount of magnetic flux, changes in the vortex density appear as an induced voltage in the pickup coil. In the presence of a small driving magnetic field this voltage provides a measure of how easily vortices move from one columnar defect to another. A Hall probe array underneath the sample measures the local magnetic field component perpendicular to the columnar defects to sense vortex rotation in response to the external magnetic field (see Fig. 2).

The three YBCO single crystals we measured were all cleaved from a single parent de-twinned sample which was polished down to approximately 35 μm (along the c axis). One was kept as a reference, and the other two were irradiated at the National Superconducting Cyclotron Laboratory at Michigan State University with 4 GeV Au ions to magnetic field equivalent densities of 0.5 and 0.25 T. The resulting microscopic damage is known to consist of randomly distributed, parallel cylindrical regions of amorphous material, approximately 70 Å (Ref. 24) in diameter which extend throughout the entire thickness of the crystal along the c axis. The three crystal platelets had a thickness of approximately 35 μm (along the c axis) and lateral dimensions of approximately 0.5×0.5 mm^2. The zero field transition temperatures ranged from 91.5 to 92.5 K with transition widths of 0.3 K as determined by ac susceptibility measurements.

The Hall probe magnetometers were fabricated from an undoped thin film of InAs epitaxially grown on a GaAs substrate.[25] Using standard photolithographic techniques we patterned a 10 probe array with each probe element separated by 10 μm and possessing an active area of 3×3 μm^2. The crystals were positioned over the array of Hall probes with the columnar defect axis (the c axis in the unirradiated crystal) perpendicular to the magnetic field sensing direction. The precise lateral position of the crystal was checked by trapping flux in the crystal and then observing the magnetic field profile with the Hall probes as shown in Fig. 1.

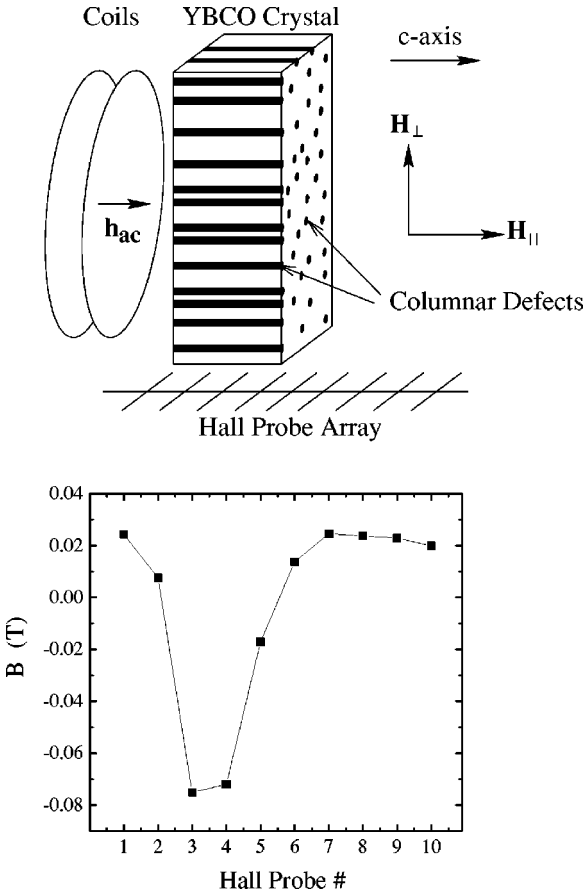

FIG. 1. Schematic of the experimental setup. The $YBa_2Cu_3O_{7-\delta}$ crystals were positioned over a Hall probe array with the columnar defects perpendicular to the magnetic field sensing direction. The position of the crystal across the Hall probes was determined by field cooling the crystal in a perpendicular magnetic field and then ramping the external field to zero. The resulting magnetic field profile indicates that the crystal is close to the Hall probes and is centered over Hall probes 3 and 4. A small pickup coil detects vortex motion perpendicular to the columns in response to a small ac drive magnetic field h_{ac} generated by coils not shown.

We identify the melting transition as the temperature and magnetic field where the sample screens a small ac magnetic field. The amplitude and phase of the resulting induced electric field in the pickup coil shows a characteristic decrease as the sample is cooled through the transition (see inset to Fig. 4). We choose as a melting criterion the temperature at which the real part of the electric field amplitude has dropped by 20% of its maximum value. This corresponds to a drop of the sample resistance to less than 1/1000 of the normal state value at a current density in the range from 1 to 10 A/cm^2. We used this criterion to minimize the induced current in the sample while still being sensitive to small changes in the melting temperature. Further, we adjusted the probing current to be in the regime of linear response. We note that an equivalent choice of melting criterion based on

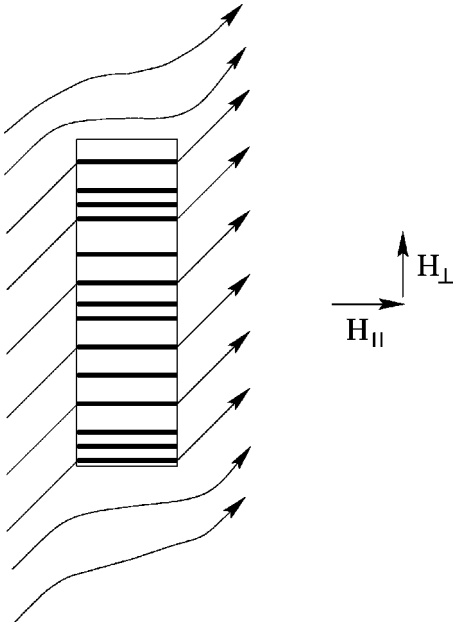

FIG. 2. Illustration of the magnetic field profile associated with the transverse Meissner effect. The external magnetic field is rotated off the columns, but the component of magnetic field perpendicular to the columns bends around the sample, leaving the local magnetic flux both inside and just underneath the crystal aligned with the defect axis.

the imaginary response is possible, and gives the same qualitative results.

III. SHAPE OF THE MELTING LINE

We first consider the melting line for the case when the magnetic field is parallel to the columnar defect axis. Due to the extreme sensitivity of the melting temperature on the magnetic field direction, the two perpendicular components of magnetic field were adjusted independently (using a three-axis split coil magnet) at each value of $\mu_0 H_\parallel$ to maximize the melting temperature. In the unirradiated sample alignment was first made to the ab plane along two orthogonal directions. The c axis was then taken as pointing in the direction offset 90° from each in-plane direction. Alignment using the latter method was only accurate to approximately one degree. However, the melting temperature in the unirradiated sample was constant for changes in the magnetic field direction on the order of 10°. We plot in Fig. 3 the parallel magnetic field $\mu_0 H_\parallel$ against the melting temperature T_m for the three crystals. As anticipated, the melting line is pushed to higher magnetic fields and temperatures by the presence of columnar defects. Another change induced by the irradiation appears in the slope $\mu_0 dH_\parallel/dT_m$ of the melting line. While $\mu_0 dH_\parallel/dT_m$ in the unirradiated sample is nearly constant except for $T/T_c \simeq 1$, there is a 30% decrease in $\mu_0 dH_\parallel/dT_m$ in the irradiated samples as the magnetic field increases through the matching field, i.e., when $\mu_0 H = B_\phi$ (see the inset to Fig. 3).

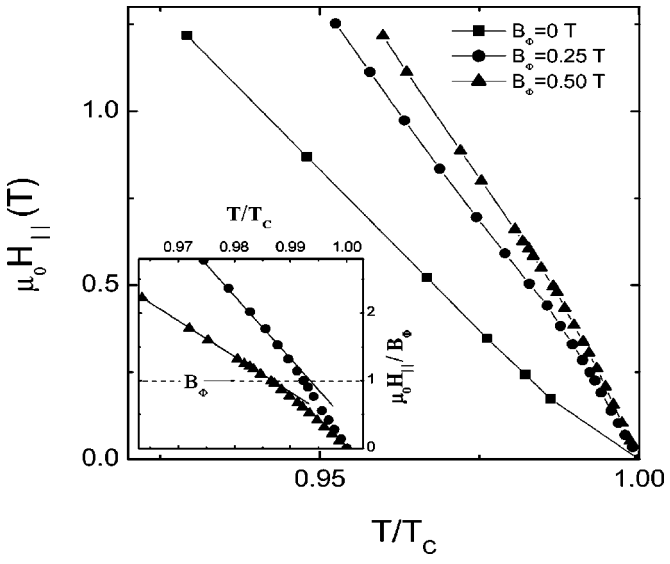

FIG. 3. Parallel magnetic field $\mu_0 H_\parallel$ vs reduced melting temperature T_m/T_c for two irradiated and one unirradiated YBCO crystal. Inset: Normalized parallel magnetic field $\mu_0 H_\parallel/B_\phi$ vs reduced melting temperature T_m/T_c.

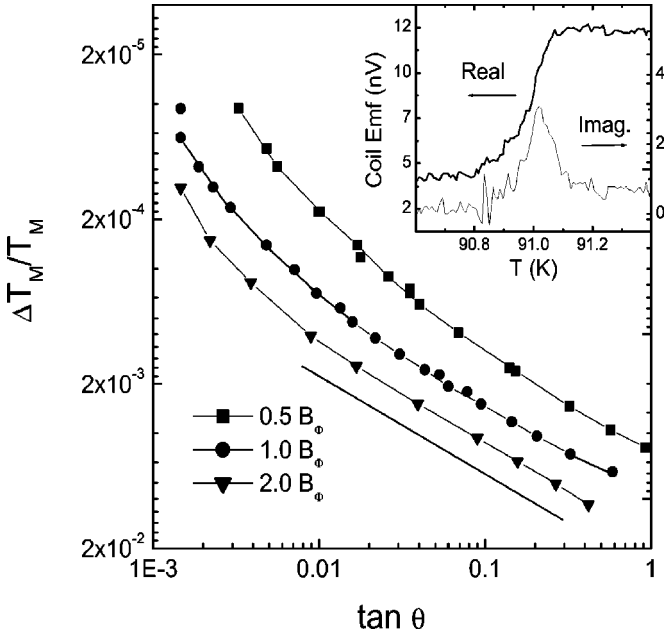

FIG. 4. Log-log plot of the relative change in vortex melting temperature $\Delta T_m/T_m = [T_m(H_\perp = 0) - T_m(H_\perp)]/T_m(H_\perp)$ vs the tangent of magnetic field angle tan θ for several values of magnetic field parallel to the columnar defects. The straight line indicates a power law dependence $\Delta T_m/T_m \propto H_\perp^{1/\nu}$ with $\nu = 1.7$. Inset: Real and imaginary part of the ac coil response. We choose the temperature where the real part of the voltage has dropped by 20% of its maximum value as the criterion for T_m.

Such a feature in the phase boundary at $B = B_\phi$ is unexpected. It is only at low temperatures where the pinning energy is sufficiently large compared to vortex-vortex interactions that NV predict the matching field acquires a special significance. In particular, they predict the formation of a Mott-insulator phase as $T \to 0$ characterized by an infinite compressional modulus at $B = B_\phi$. Evidence of such a phase has been observed in recent experiments on magnetization

relaxation.[26] While the change in slope we observe is not indicative of an incompressible vortex phase extending to high temperatures, it does indicate that interstitial vortices are caged (or collectively pinned) only weakly compared to those occupying columnar defects. In this case there should be few interstitials until all the columnar defects are occupied by vortices. Recent theoretical[27,28] approaches have revisited this problem and find characteristic changes in the melting line at the matching field. Radzihovsky[27] argues that the presence of interstitial vortices should lead to a weakly pinned Bose glass phase characterized by rapid decrease in T_m with increasing interstitial vortex density. However, the precise form of the decrease is estimated only in the limit of small matching fields ($B_\phi \sim \mu_0 H_{c_1}$) and is inconsistent with the linear behavior we observe above the matching field. Larkin and Vinokur[28] discuss the additional limit $B_\phi \gg \mu_0 H_{c_1}$ and argue that the maximum enhancement in T_m due to disorder should occur near the matching field B_ϕ, where the constraining effects of nearby vortices enhance the confinement of the pinning potential. However, in Fig. 3 the enhancement of T_m becomes increasingly larger with increasing B and does not show any sign of saturating even as B exceeds $2B_\phi$. Experimental reports as to the shape of the melting line in YBCO also vary.[15,18,29–32] While Refs. 18 and 29 report a change of slope at B_ϕ, the others report either no feature[32] at the matching field or else a change of slope, but at a smaller fraction of the matching field.[31]

Next we consider the melting line as the magnetic field is rotated off the direction set by the columns. We plot in Fig. 4 T_m as a function of the perpendicular magnetic field for the 0.25 T crystal. As expected, T_m decreases as the magnetic field is rotated off the defect axis. Furthermore, the reduction in T_m is observable for rotations of the magnetic field as small as 0.1° and continues to decrease substantially out to angles as large as 45°. According to theory,[7] the Bose glass should be suppressed as $T_{BG}(H_\perp = 0) - T_{BG}(H_\perp) \propto H_\perp^{1/\nu_\perp}$, where $\nu_\perp$ is the static critical exponent describing the transition for **H** parallel to the columnar defects. Over two decades of angle on a log-log plot, $\tan\theta = 0.01$ to 1, the data do follow a line, indicating power law behavior. However, at small angles below about one degree an upward curvature develops. We do not know whether this represents a change in the intrinsic behavior for small angles or whether it is an artifact due to splay in the columnar defect axis. If we assume the latter, the data are consistent with an exponent $\nu_\perp = 1.7 \pm 0.2$. This result is considerably larger than the expected value determined from simulations of 2D bosons subject to point disorder where $\nu_\perp \simeq 1$. Alternatively, the behavior for $\tan\theta < 0.01$ may indicate a crossover at small angles to a value of $\nu_\perp$ closer to 1. The melting temperature shows similar behavior (including the upward curvature at small angle) in the case of the 0.5 T sample except for a slightly larger exponent, $\nu_\perp = 1.9 \pm 0.1$.

IV. TRANSVERSE MEISSNER EFFECT

The second fundamental property of the Bose glass is the presence of a transverse Meissner effect below the melting temperature. As a first step to test this prediction directly, we cooled the sample in a magnetic field parallel to the columnar defects. Alignment was again taken to be the magnetic field direction which maximized the melting temperature. We then ramped a perpendicular magnetic field with the Hall probes recording the magnetic field profile underneath the crystal. A transverse Meissner effect should result in a reduction in the perpendicular component of magnetic field underneath the crystal (see Fig. 2) regardless of the sign of $H_\perp$. To demonstrate this effect, we consider the perpendicular magnetization $M_\perp$, taken as the difference between the perpendicular magnetic field $B_\perp$ underneath the sample and the component $H_\perp$ of the applied field. We show in Fig. 5 $M_\perp$ for both an irradiated and unirradiated crystal as the applied field $H_\perp$ was swept through cycles $H_\perp^{\max} \rightarrow -H_\perp^{\max} \rightarrow H_\perp^{\max}$

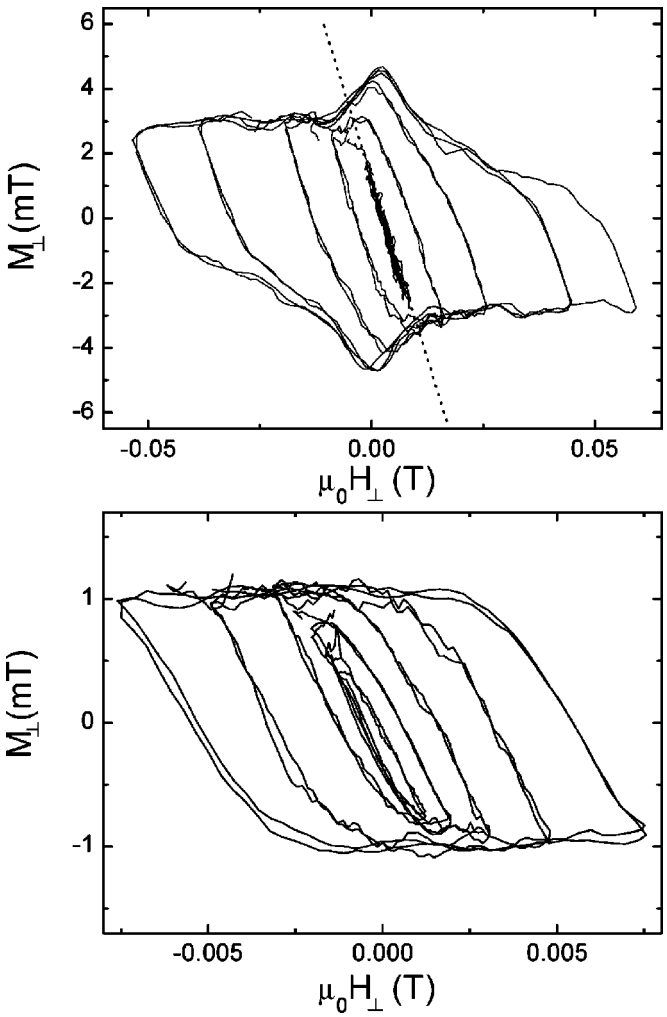

FIG. 5. Transverse magnetization $M_\perp$ vs perpendicular magnetic field $H_\perp$ for fixed $\mu_0 H_\parallel = 0.21$ T and temperature $T = 65$ K. $H_\perp$ cycles from $H_\perp^{\max} \rightarrow -H_\perp^{\max} \rightarrow H_\perp^{\max}$ where $H_\perp^{\max}$ is increased after each cycle. In the irradiated crystal (top panel) the magnetization loops show no hysteresis for $H_\perp^{\max}$ less than $H_\perp^c$ and lie on the dashed line, indicating that the field lines remain parallel to the columnar defects (transverse Meissner effect). The unirradiated crystal (bottom panel), by contrast, shows hysteresis even for relatively small $H_\perp^{\max}$, as expected for unscreened penetrating flux.

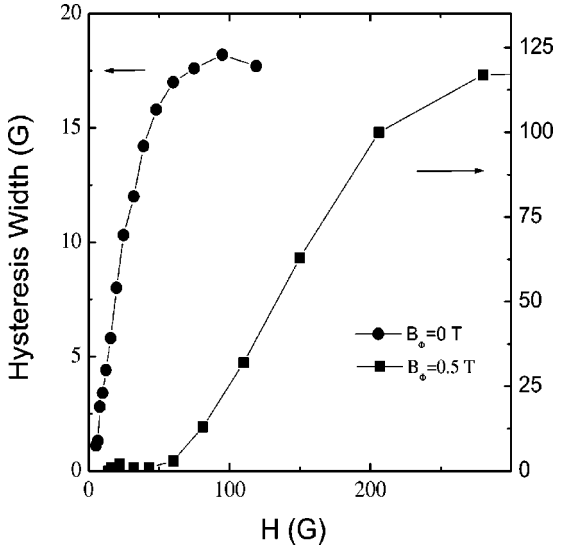

FIG. 6. Average hysteresis width vs amplitude of field ramp $H_\perp^{\max}$ for Hall probes positioned directly underneath the crystal, measured at $T=65$ K and $\mu_0 H_\parallel = 0.2$ T. The hysteresis width was determined from plots of $B_\perp(H_\perp)$, averaged over a cycle. In the irradiated crystal the hysteresis width remains negligible up to a threshold field $H_\perp^c$, which we identify with the breakdown of transverse flux screening. The unirradiated crystal shows hysteresis down to $H_\perp \approx 0$.

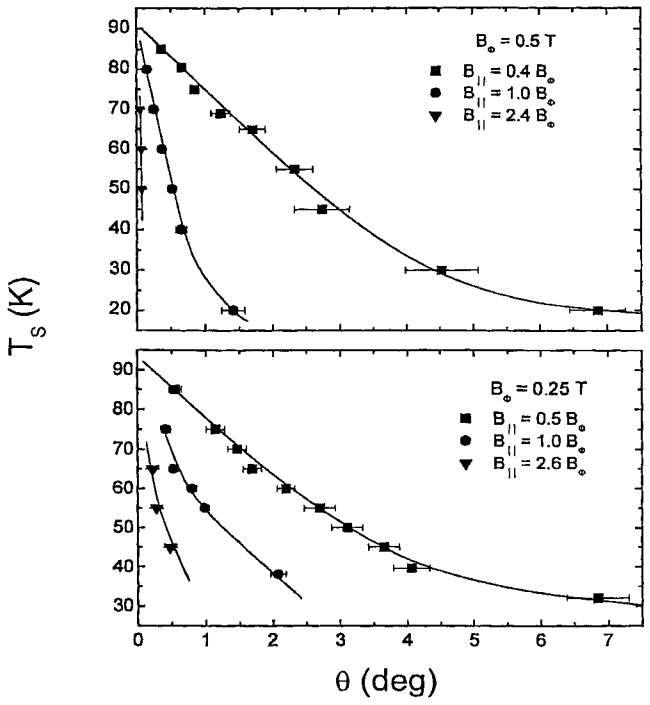

FIG. 7. Screening temperature $T_s(H_\perp)$ vs the magnetic field angle θ for several values of normalized parallel magnetic field $\mu_0 H_\parallel / B_\phi$ for the two irradiated crystals.

with successively increasing ramp end points $\pm H_\perp^{\max}$. In the irradiated crystal for small $H_\perp^{\max}$, we find $M_\perp \propto -H_\perp$ and negligible hysteresis. These two results taken together indicate that the superconductor screens the component of applied field perpendicular to the columnar defects. At sufficiently large $H_\perp^{\max}$, $M_\perp$ abruptly becomes hysteretic and is no longer proportional to $-H_\perp$. For larger $H_\perp^{\max}$, $M_\perp$ decreases even further relative to the dashed line (indicating that the magnetic field direction rotates further away from the columnar defect direction) and the transverse Meissner effect is lost. By comparison, the unirradiated sample shows hysteretic behavior even for small values of $H_\perp^{\max}$. A lock-in effect showing similar behavior has also been observed[16] in twinned YBCO samples indicating the general nature of the effect.

In order to determine $H_\perp^c$, the field at which transverse flux enters the superconductor, we measured the hysteresis in the local field under the sample, $B_\perp$, as a function of $H_\perp^{\max}$. We plot in Fig. 6 the average hysteresis width of the resulting magnetization loops $B_\perp(H_\perp)$. In the irradiated samples, this width is seen to remain negligible until $H_\perp$ reaches a critical value $H_\perp^c$, beyond which it increases sharply. The hysteresis width measured in the unirradiated crystal at the same temperature and at the same parallel magnetic field shows almost no offset in $H_\perp$. There is a small residual offset in the unirradiated crystal. When normalized to the value of $H_\perp$ at which the hysteresis width saturates, it is less than 20% of that in the irradiated sample, and it is even smaller in absolute value. We note that in both cases the hysteresis width increases approximately linearly in $H_\perp$ before saturating. This is consistent with a simple Bean profile for the entering transverse flux.

In addition to flux screening, there should also be flux expulsion upon field cooling into the transverse Meissner state. However, we do not expect to observe this since hysteresis develops once flux enters the superconductor. As in conventional measurements of H_{c1}, point pinning effects prevent a precise determination of the thermodynamic state. Possible comparisons of field cooled and zero field cooled protocols very near T_c (where point pinning is weaker) demand sensitivity beyond the capabilities of the experiment.

Our direct observation of flux screening validates a central prediction of the Bose glass theory. Moreover, from measurements of the critical transverse field $H_\perp^c(T)$, we can define a maximum screening temperature $T_s(H_\perp)$ above which the transverse Meissner effect breaks down. Figure 7 shows T_s as a function of tilt angle $\theta \equiv H_\perp / H_\parallel$. In both irradiated crystals T_s decreases linearly with increasing θ over a range of many tens of kelvin within the first 3° of field tilt. For $\mu_o H_\parallel \simeq 2.5 B_\Phi$, where each columnar defect must hold on to more than one vortex, T_s falls even more rapidly, dropping by 50% before θ reaches 0.5°. The rate of decrease in T_s with angle is greatest in the sample with the largest defect density, and this difference is most pronounced for $B > B_\phi$.

We compare in Fig. 8 the two irradiated crystals measured at similar values of $\mu_0 H_\parallel = 0.2$ T, well below their matching fields. At these low fields there are more columnar defects than vortices. Here we see the opposite trend: $T_s(H_\perp)$ is greatest in the sample with the largest defect density. Presumably the larger choice of pinning sites allows the vortices

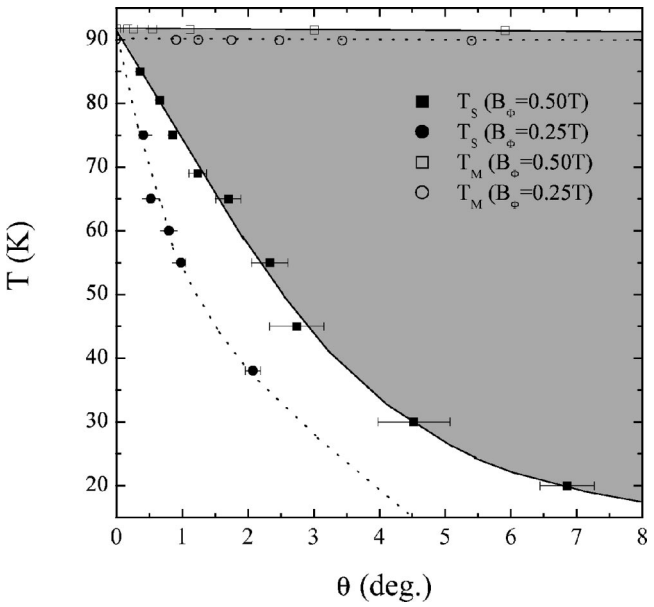

FIG. 8. Flux screening $T_s(H_\perp)$, filled symbols, and melting $T_m(H_\perp)$, open symbols, temperatures vs the magnetic field angle θ for $\mu_0 H_\parallel \simeq 0.2$ T. T_s falls off most rapidly for the sample with the smaller irradiation dose. T_s approaches T_m as $\theta \to 0$, but at relatively small angles they rapidly diverge. There is an unexpected intermediate regime where vortices are immobilized by the columnar disorder but track the external magnetic field direction (note the expected cusp in T_m as a function of angle is present but not noticeable on this temperature scale).

to be farther apart and therefore implies a smaller interaction potential. In turn, this may increase the effective pinning energy per unit length, leaving the vortices more resistant to tilt. In the case of the unirradiated crystal we find little if any transverse Meissner effect for $T > 50$ K. At lower T, a small effect appears. We attribute this to the intrinsic anisotropy of YBCO coupled with point disorder. According to Ref. 33, an anisotropic superconductor such as YBCO can be mapped onto an isotropic one which is stretched spatially along the c axis. In this mapping, point defects become elongated and should exhibit the strongest pinning for magnetic fields aligned with them. At low temperatures, where the pinning is strongest, many of these defects may conspire to hold vortices parallel to the c axis and therefore induce a transverse Meissner effect. This scenario is consistent with the increase of θ^c only at low temperatures where the effect of point disorder is most significant. Interestingly a similar increase of θ^c occurs at the same temperature in the irradiated samples. We speculate that point disorder may contribute to the enhancement independent of the columnar defect density. However, we cannot rule out the possibility that residual twin planes exist in our samples. The YBCO crystals measured were determined to be twin free by examining them with a polarized-light optical microscope, thus they contained many fewer twin defects than untwinned samples. Such residual twin planes or other extended defects like screw dislocations could account for our observation of a small transverse Meissner effect in the unirradiated crystal.

V. COMPARISON OF MELTING AND TRANSVERSE FLUX SCREENING

We compare in Fig. 8 measurements of the screening temperature T_s, with measurements of the angular dependence of the melting temperature, T_m. On the same temperature scale, T_m changes negligibly in comparison to T_s. It is only as $\theta \to 0$ that T_s approaches T_m. Otherwise, the two temperatures rapidly depart already at small angles (for example, at 3°, the difference exceeds 50 K). We note that other reports of the dependence of T_m on magnetic field direction found in the literature[10,13,19,34,35] would be difficult to distinguish from our measurements if plotted on the same scale. Typically, T_m is found to decrease by a few kelvin for large rotations (on the order of tens of degrees) of the magnetic field and is never comparable to the precipitous drop we measure for T_s. The divergence of $T_m(\theta)$ and $T_s(\theta)$ presents a conundrum. The angular dependence of the melting temperature T_m signifies the important role played by columnar defects. However, vortices become immobile out to large angles and at temperatures where they are no longer aligned with the columnar defects. If we identify T_s rather than T_m with the Bose-glass transition temperature, T_{BG}, then we find a static critical exponent $\nu = 1.0 \pm 0.1$ for $\mu_0 H_\parallel \simeq 0.5 B_\phi$ and $\mu_0 H_\parallel \simeq 1.0 B_\phi$. This value of ν is at the lower boundary of the inequality $\nu \geqslant 2/d$,[36] with system dimensionality $d = 2$, and it agrees with recent computer simulations.[22]

Further evidence that T_s may be the appropriate demarcation of the Bose glass comes from the disparity in the magnitudes of T_s and T_m. Energetically, it is unfavorable for T_s to track the melting temperature out to such large angles. According to Ref. 7 the critical field angle is

$$\theta^c = \frac{\sqrt{\epsilon_l U_o}}{\phi_o H_\parallel},$$

where ϵ_1 is the line energy per vortex and U_o is the pinning energy per unit length. Using the relations

$$\epsilon_1 \simeq \gamma^2 \frac{\phi_o^2}{4\pi\mu_o \lambda^2} \ln a_o / \xi_{ab}$$

and

$$U_o \simeq 0.5 \frac{\phi_o^2}{4\pi\mu_o \lambda^2} \ln\left[1 + \left(\frac{c_o}{\xi_{ab}\sqrt{2}}\right)^2\right],$$

where $\lambda = 1700$ Å is the in-plane magnetic penetration depth, $\xi_{ab} = 12$ Å is the in-plane coherence length, $\gamma^2 \simeq 64$ is the mass anisotropy ratio and $a_o \simeq 770$ Å (for $B = 0.25$ T) is the average vortex spacing, we find $\theta^c \simeq 0.1°$. This value is about one order of magnitude smaller than θ^c determined by flux screening and several orders of magnitude below that determined by vortex melting.

We find strong evidence of a Bose glass phase at low temperatures and small tilt angles. Here, vortices are truly aligned with the columnar defects and are clearly immobilized. In particular, we have directly demonstrated that transverse flux is screened out in this region of $H_\perp, T$ phase

space. On the other hand, above T_m vortices are clearly in a mobile, liquid state, characterized by finite resistivity and large transverse flux penetration.

The nature of the vortex phase in the temperature range $T_m(\theta) > T > T_s(\theta)$ (shaded region in Fig. 8) remains an open question. In this large region of phase space, translational degrees of freedom are well frozen, but rotation off the direction set by the columnar defect axes apparently is possible. One might be tempted to argue that this phase is simply a vortex glass dominated by point disorder, i.e., that the columnar defects might have been rendered ineffective by tilting the magnetic field. However, this scenario cannot explain the strong angular dependence we observe in the melting temperature T_m, which clearly indicates that the columnar defects remain effective out to very large angles (Fig. 4). Instead, we speculate that the zero resistance phase results from crossing vortex line segments (or vortex ''kinks'') which connect vortices on different columnar defects.[37,38] Finally, there is the possibility that $T_m(\theta)$ and $T_s(\theta)$ cannot be accounted for within the currently available Bose glass models. These models predict a single phase boundary between the vortex liquid and the solidlike, glassy phase. In related 2D bosonic systems, this would correspond to a direct transition from the superconductor or superfluid into the insulating phase. However, there is mounting experimental evidence[39] for an intervening metallic phase in a two-stage superconductor-metal-insulator transition. The additional vortex phase found in this work may be another example of such an intervening region in phase space.

In the absence of general predictions for the structure of vortex matter in the intermediate phase, it is instructive to consider some tentative, specific possibilities. The fact that vortices in this regime unlock from the columnar defects yet remain localized may be understood in terms of a highly anisotropic ''correlated vortex glass'' state proposed by Radzihovsky.[40] In this state the vortex flux bundles experience the columns as an effective, tilt-dependent point disorder. This interpretation also would predict a highly anisotropic resistivity, controlled by the columnar defect density and any residual point disorder. At large tilt angles, the correlated vortex glass would be expected to turn into a ''smectic glass'' characterized by two Bragg spots for scattering along the columnar defect axis rather than the six spots corresponding to a triangular lattice. This prediction could be checked by neutron scattering.

ACKNOWLEDGMENTS

We are grateful to S. Kivelson, D.R. Nelson, and L. Radzihovsky for insightful comments and to A.M. Petrean for help in sample preparation. This work was supported by the National Science Foundation through the Science and Technology Center for Superconductivity (DMR91-20000) and by the MRSEC Program of the NSF under Grant No. DMR-9808595. W.K.K. and G.W.C. acknowledge additional support by the U.S. Department of Energy, Office of Science/Basic Energy Science under Contract No. W-31-109-ENG-38.

[1] For a review, see G. Blatter, M.V. Feigel'man, V.B. Geshkenbein, A.I. Larkin, and V.M. Vinokur, Rev. Mod. Phys. **66**, 1125 (1994).

[2] A. Schilling, R.A. Fisher, N.E. Phillips, D. Dasgupta, U. Welp, W.K. Kwok, and G.W. Crabtree, Nature (London) **382**, 791 (1996).

[3] J.A. Fendrich, W.K. Kwok, J. Giapintzakis, C.J. van der Beek, V.M. Vinokur, S. Fleshler, U. Welp, H.K. Viswanathan, and G.W. Crabtree, Phys. Rev. Lett. **74**, 1210 (1995).

[4] K. Deligiannis, P.A.J. de Groot, M. Oussena, S. Pinfold, R. Langan, R. Gagnon, and L. Taillefer, Phys. Rev. Lett. **79**, 2121 (1997).

[5] L.M. Paulius, W.K. Kwok, R.J. Olsson, A.M. Petrean, V. Tobos, J.A. Fendrich, G.W. Crabtree, C.A. Burns, and S. Ferguson, Phys. Rev. B (to be published).

[6] D.S. Fisher, M.P.A. Fisher, and D.A. Huse, Phys. Rev. B **43**, 130 (1991).

[7] D.R. Nelson and V.M. Vinokur, Phys. Rev. B **48**, 13 060 (1993).

[8] M.P.A. Fisher, P.B. Weichman, G. Grinstein, and D.S. Fisher, Phys. Rev. B **40**, 546 (1989).

[9] L. Civale, A.D. Marwick, T.K. Worthington, M.A. Kirk, J.R. Thompson, L. Krusin-Elbaum, Y. Sun, J.R. Clem, and F. Holtzberg, Phys. Rev. Lett. **67**, 648 (1991).

[10] W. Jiang, N.-C. Yeh, D.S. Reed, U. Kriplani, D.A. Beam, M. Konczykowski, T.A. Tombrello, and F. Holtzberg, Phys. Rev. Lett. **72**, 550 (1994).

[11] L. Krusin-Elbaum, L. Civale, G. Blatter, A.D. Marwick, F. Holtzberg, and C. Feild, Phys. Rev. Lett. **72**, 1914 (1994).

[12] R.C. Budhani, W.L. Holstein, and M. Suenaga, Phys. Rev. Lett. **72**, 566 (1994).

[13] D.S. Reed, N.-C. Yeh, M. Konczykowski, A.V. Samoilov, and F. Holtzberg, Phys. Rev. B **51**, 16 448 (1995).

[14] C.J. van der Beek, M. Konczykowski, V.M. Vinokur, T.W. Li, P.H. Kes, and G.W. Crabtree, Phys. Rev. Lett. **74**, 1214 (1995).

[15] G. Nakielski, A. Rickertsen, T. Steinborn, J. Wiesner, G. Wirth, A.G.M. Jansen, and J. Kötzler, Phys. Rev. Lett. **76**, 2567 (1996).

[16] M. Oussena, P.A.J. de Groot, K. Deligiannis, A.V. Volkozub, R. Gagnon, and L. Taillefer, Phys. Rev. Lett. **76**, 2559 (1996).

[17] C. Reichhardt, C.J. Olson, J. Groth, Stuart Field, and Franco Nori, Phys. Rev. B **53**, R8898 (1996).

[18] A. Mazilu, H. Safar, M.P. Maley, J.Y. Coulter, L.N. Bulaevskii, and S. Foltyn, Phys. Rev. B **58**, R8909 (1998).

[19] S.A. Grigera, E. Morré, E. Osquiguil, C. Balseiro, G. Nieva, and F. de la Cruz, Phys. Rev. Lett. **81**, 2348 (1998).

[20] M. Wallin and S. Girvin, Phys. Rev. B **47**, 14 642 (1993).

[21] D.R. Nelson and L. Radzihovsky, Phys. Rev. B **54**, R6845 (1996).

[22] J. Lidmar and M. Wallin, Europhys. Lett. **47**, 494 (1999).

[23] I.M. Obaidat, S.J. Park, H. Safar, and S. Kouvel, Phys. Rev. B **56**, R5774 (1997).

[24] Y. Yan and M.A. Kirk, Phys. Rev. B **57**, 6152 (1998).

[25] E. Pugel, E. Shung, T.F. Rosenbaum, and S.P. Watkins, Appl. Phys. Lett. **71**, 2205 (1997).

[26] K.M. Beauchamp, T.F. Rosenbaum, U. Welp, G.W. Crabtree, and V.M. Vinokur, Phys. Rev. Lett. **75**, 3942 (1995); E.R. Nowak, S. Anders, H.M. Jaeger, J.A. Fendrich, W.K. Kwok, R. Mogilevsky, and D.G. Hinks, Phys. Rev. B **54**, R12 725 (1996).
[27] L. Radzihovsky, Phys. Rev. Lett. **74**, 4923 (1995).
[28] A.I. Larkin and V.M. Vinokur, Phys. Rev. Lett. **75**, 4666 (1995).
[29] W.K. Kwok, L. Paulius, D. Lopez, H. Safar, R.J. Olsson, A.M. Petrean, and G.W. Crabtree, Mater. Sci. Forum **315-317**, 314 (1999).
[30] T.K. Worthington, M.P.A. Fisher, D.A. Huse, J. Toror, A.D. Marwick, T. Zabel, and C.A. Feild, Phys. Rev. B **46**, 11 854 (1992).
[31] L. Krusin-Elbaum, L. Civale, G. Blatter, A.D. Marwick, F. Holtzberg, and C. Feild, Phys. Rev. Lett. **72**, 1914 (1992).
[32] A.V. Samoilov, M.V. Feigel'man, M. Konczykowski, and F. Holtzberg, Phys. Rev. Lett. **76**, 2798 (1996).
[33] G. Blatter, V.B. Geshkeinbein, and A.I. Larkin, Phys. Rev. Lett. **68**, 875 (1992).
[34] L.M. Paulius, J.A. Fendrich, W.K. Kwok, A.E. Koshelev, V.M. Vinokur, G.W. Crabtree, and B.G. Glagola, Phys. Rev. B **56**, 913 (1997).
[35] A.W. Smith, H.M. Jaeger, T.F. Rosenbaum, W.K. Kwok, and G.W. Crabtree, Phys. Rev. B **59**, R11 665 (1999).
[36] J.T. Chayes, L. Chayes, D.S. Fisher, and T. Spencer, Phys. Rev. Lett. **57**, 2999 (1986).
[37] G. Blatter, J. Rhyner, and V.M. Vinokur, Phys. Rev. B **43**, 7826 (1991).
[38] E.B. Sonin, Phys. Rev. B **48**, 10 487 (1993).
[39] E. Shimshoni, A. Auerbach, and A. Kapitulnik, Phys. Rev. Lett. **80**, 3352 (1998).
[40] L. Radzihovsky (private communication).